Optical anisotropy in GaAs/AlAs (110) superlattices

U. Schmid
Max-Planck-Institut für Festkörperforschung, Heisenbergstrasse 1, D-7000 Stuttgart 80, Germany

N.E. Christensen
Max-Planck-Institut für Festkörperforschung, Heisenbergstrasse 1, D-7000 Stuttgart 80, Germany and Institute of Physics, Aarhus University , DK-8000 Aarhus C, Denmark

M. Cardona, F. Lukeš,* and K. Ploog†
Max-Planck-Institut für Festkörperforschung, Heisenbergstrasse 1, D-7000 Stuttgart 80, Germany
(Received 21 August 1991)

Short-period GaAs/AlAs superlattices grown along the [110] direction have orthorhombic symmetry and thus exhibit two different dielectric functions $\epsilon(\omega)$ along the main axes perpendicular to the growth direction ([001] and [1$\bar{1}$0] direction). Spectroscopic ellipsometry as well as *ab initio* calculations have been used to determine the optical properties of these superlattices. The E_1 transitions split into two components with different strengths for the two principal polarizations. This effect can be qualitatively interpreted on the basis of a $\mathbf{k}\cdot\mathbf{p}$ model for the E_1 transitions and confinement arguments. The E_2 transition for [001] polarization is lower in energy than the one for [1$\bar{1}$0] polarization. In addition, we observe a transition slightly above E_2, which occurs predominantly in [001] polarization. Two other structures specific to the superlattices are identified, in analogy to the case GaAs/AlAs superlattices grown along [001]. Confinement effects on optical transitions for various superlattice periods are also discussed.

The linear optical properties of short-period GaAs/AlAs superlattices (SL's) grown along the [001] direction have been studied in detail with both theoretical[1–3] as well as experimental[1,4–6] methods. The effects of the additional periodicity have been shown to be important for the dielectric response, producing two structures that are specific to the superlattice[1] and which are thus not found in $Al_xGa_{1-x}As$ alloys.[7] Lately, the growth of device-quality GaAs on (110) oriented surfaces[8] and GaAs/AlAs (110) superlattices[9] by molecular beam epitaxy (MBE) and Raman studies of these superlattices[9,10] have been reported. Recent photoluminescence experiments on (110)-oriented quantum wells show an in-plane polarization anisotropy of the lowest optical transitions.[11] The GaAs/AlAs (110) superlattices are of importance for many applications, such as avalanche devices and optical modulators for integrated optics (see Ref. 8 and references therein). In addition, the nonpolar (110) GaAs surface is known to produce no intrinsic surface states in the fundamental band gap and thus makes it a preferred orientation for the growth of polar-nonpolar interface (e.g., Si on GaAs) systems.[12]

Theoretical work on GaAs/AlAs (110) SL's has focused on the electronic band structure and the crossover from a direct to an indirect gap[13,14] and on the stability of these SL's.[15,16] Here, we present both a theoretical and an experimental study of the dielectric functions of $(GaAs)_n/(AlAs)_m$ (110) SL's with emphasis on the orthorhombic anisotropy, which does not occur in GaAs/AlAs SL's grown along the [001] direction. The latter have tetragonal symmetry (optically uniaxial) and thus only two different tensor components of the dielectric function $\epsilon(\omega)$. The SL's grown along the [110] direction, however, have orthorhombic symmetry,[9] and of the three components of the dielectric function the two perpendicular to the growth direction along the main axes ([001] and [1$\bar{1}$0] directions) are experimentally accessible, whereas for light polarized along the growth direction ([110]), the small thickness of the MBE-grown samples inhibits measurement. For this reason we will not pursue the latter any more, but rather concentrate on the in-plane anisotropy, i.e., on $\epsilon_2^{[001]}$ and $\epsilon_2^{[1\bar{1}0]}$.

We will demonstrate that this anisotropy reveals itself in a splitting of the E_1 transition with different amplitudes for the two polarizations. The experiment is in qualitative agreement with a simple theoretical model of confinement of these transitions, based on $\mathbf{k}\cdot\mathbf{p}$ arguments. The difference of $\epsilon_2(\omega)$ for the two polarizations, as calculated from first principles with the linear-muffin-tin-orbitals (LMTO) method, also agrees well with experiment, although spin-orbital (s.o.) interaction is neglected in the calculation. A shift of the E_2 transition between the two polarizations is observed both experimentally and theoretically. In addition, a distinctive peak just above E_1 that is unique for light polarized along the [001] direction is detected.

The 0.5-μm-thick samples were grown by MBE on slightly misoriented (110) surfaces of GaAs in order to obtain atomically smooth interfaces, as described in more detail in Ref. 10. The periods of these SL's were obtained

from measurements with a high-resolution double-crystal x-ray diffractometer. The samples were measured with a rotating analyzer ellipsometer[7] at room temperature in the energy range 1.6–5.5 eV for the two azimuthal orientations. The effects of an oxide overlayer have been removed numerically by calculating $\epsilon_2(\omega)$ with a three-phase model[17] with tabulated values for the GaAs oxide (assumed to be isotropic).[18] The two dielectric components, which are mixed by the ellipsometric measurement technique, have been separated by a numerical inversion routine. For the purpose of this inversion, the dielectric component perpendicular to the surface, which has small influence on the measurement,[19] is assumed to be comparable to the two in-plane components, which is supported by the calculation. The magnitude of this correction to the measured dielectric components turned out to be rather small, as expected from a first-order approximation.[19]

Below 2.5 eV, the absorption of the SL's is so small that the spectra are dominated by interferences originating

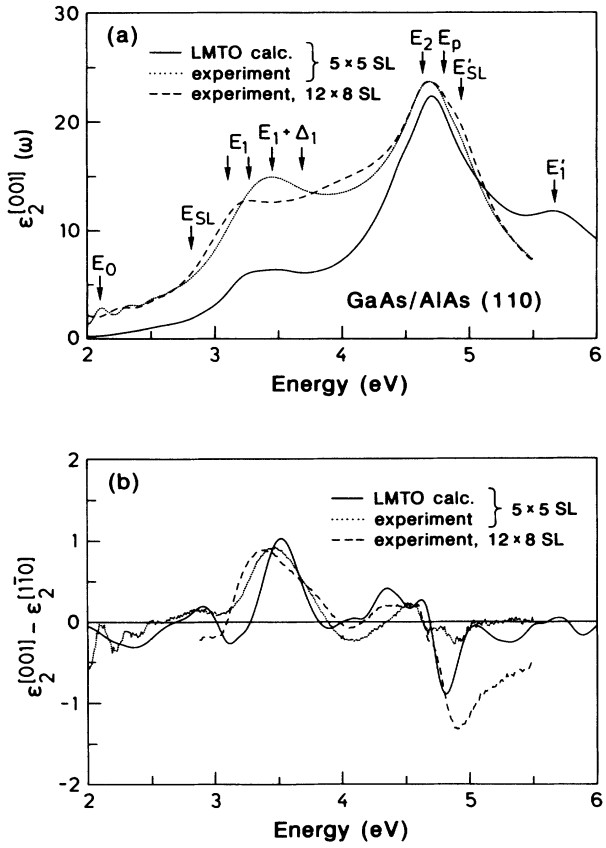

FIG. 1. (a) Imaginary part of the dielectric function for light polarized along the [001] direction in [110]-oriented superlattices. The solid line represents the result from a fully relativistic LMTO calculation for a $(GaAs)_5/(AlAs)_5$ superlattice, which can be directly compared to the experiment (dotted line). Dashed line: experimental result for a $(GaAs)_{12}/(AlAs)_8$ SL. The arrows indicate the critical points of the 5 × 5 structure. (b) Difference of the $\epsilon_2(\omega)$'s for light polarized along the [001] and [110] direction of the SL's shown in (a).

from light reflected from the SL/GaAs bulk interface.[4] This is shown in Fig. 1(a), where the imaginary part of the dielectric function for light polarized along the [001] direction, $\epsilon_2^{[001]}$, is displayed for a $(GaAs)_5/(AlAs)_5$ (dotted line) and a $(GaAs)_{12}/(AlAs)_8$ (dashed line) sample. A sudden reduction in the amplitude of the oscillations is directly related to the onset of a strong absorption edge, i.e., the first strong direct gap (E_0), in the SL's, which we found to be $\approx$ 2.1 and 2.0 eV, respectively, for the 5 × 5 and 12 × 8 structure. In Fig. 1(a), the experimental $\epsilon_2^{[001]}$ of the 5 × 5 superlattice can be directly compared to the results of the self-consistent relativistic LMTO calculation[16,20] (solid line). This method is based on the local-density approximation (LDA), which is known to notoriously underestimate the band gaps when these are derived directly as LDA eigenvalue differences. While this deficiency can, in principle, be overcome by including many-body correlations in the form of the GW-approximation[21] into the calculation, this is only possible for smaller systems than the ones studied here due to the enormous computational effort involved in such calculations. We thus add sharply peaked, external potentials on the atomic sites in the self-consistent iteration scheme.[1,20] The strengths of these *ad hoc* potentials have been chosen such[22] that the band gaps in bulk GaAs and AlAs agree with experimental data at 4 K. In the calculation of the dielectric function,[23] the **k**-space integration has been performed by means of the tetrahedron method.[24] In order to reproduce fine details of $\epsilon_2(\omega)$, such as the anisotropy $\perp$ [110], a rather large number of **k** points has to be used: for the 5 × 5 structure displayed in Fig. 1 (solid line), 560 **k** points in the irreducible part of the Brillouin zone (BZ) were used. For the 7 × 7 structure, 352 **k** points were the maximum we could use in order not to exceed our computational resources.

For better comparison with experiment, we simulate the effects of lifetime broadening on the various transitions by folding the calculated spectra with a Lorentzian of Γ=0.15 eV full width at half maximum. This value yielded the best overall agreement in the whole spectral range with the experiment and is also typical for most transitions in $Al_xGa_{1-x}As$ alloys and the two constituting bulk materials at room temperature.[7] The same procedure has been used to identify structures in strained short-period Ge/Si superlattices.[25]

We see in Fig. 1(a) qualitative agreement between the experimental (dotted line) and calculated (full line) $\epsilon_2^{[001]}(\omega)$ of the 5 × 5 SL. As in the bulk materials, the calculated magnitude of the E_1 transitions is underestimated due to the neglect of excitons and other many-body phenomena.[23] The difference of $\epsilon_2(\omega)$ for light polarized along the [001] and [1$\bar{1}$0] direction is shown in Fig. 1(b). Here, the agreement between calculation and experiment is excellent for the energy region around E_1—the main difference for the two polarizations occurs at $\approx$3.4–3.5 eV, i.e., slightly above the E_1 transitions. The anisotropy at higher energies is not so pronounced for the 5 × 5 sample, which is probably due to sample imperfections such as interface alloying. For the 12 × 8 sample, however, the effect is rather strong with the major dis-

similarity appearing at 4.9 eV, which coincides with the additional superlattice transition E'_{SL} discussed later.

Let us first concentrate on the effects on the E_1 transitions caused by growing the superlattices along the [110] direction and thus reducing the symmetry. It is possible to perform a model calculation based on confinement and $\mathbf{k}\cdot\mathbf{p}$ arguments which displays, in a simple physical way, the possible origin of the [001]-[1$\bar{1}$0] optical anisotropy. We argue as follows. The E_1 and $E_1+\Delta_1$ transitions of bulk zinc-blende-type semiconductors are well known to be related to critical lines (two-dimensional critical points) along the four equivalent ⟨111⟩ directions. The corresponding initial and final bands around these critical points can be represented by simple analytical expressions with only the critical point energies E_1, $E_1+\Delta_1$ and the matrix element of $\mathbf{p}$ transverse to any of the ⟨111⟩ directions ($\langle s|p_{\bar{X}}|\bar{X}\rangle \simeq 2\pi/a_0$, where a_0 is the lattice constant).[26]

Within the standard analytical model the reduced longitudinal (i.e., parallel to a given ⟨111⟩ direction) masses of the E_1 and $E_1+\Delta_1$ critical points are infinite (i.e., valence and conduction bands are parallel). This enables us to treat these critical points as "critical lines" or two-dimensional critical points. Consequently, confinement effects will only take place for a given ⟨111⟩ direction if it has a component in the confinement plane. We assume infinite potential barriers bearing in mind that this will overemphasize confinement effects. For a slab perpendicular to [110] the four ⟨111⟩ directions fall into two categories (i.e., two different angles α between them and [110]):

$$[111],[1\bar{1}\bar{1}](\cos^2\alpha=\tfrac{2}{3})$$
$$\text{and} \qquad (1)$$
$$[\bar{1}1\bar{1}],[1\bar{1}\bar{1}](\cos^2\alpha=0)\ .$$

We treat first the case $\Delta_1 \neq 0$. The confinement effects for infinite barriers are given by

$$\Delta E=\begin{cases}1/4m_{c\perp}(\pi/d)^2 & \text{for } [111],[\bar{1}\bar{1}1]\\ 3/4m_{c\perp}(\pi/d)^2 & \text{for } [\bar{1}1\bar{1}],[1\bar{1}\bar{1}]\ ,\end{cases} \qquad (2)$$

where $m_{c\perp}$ is the conduction-band mass perpendicular to the [111] direction and we have made use of the fact that the corresponding valence masses are $m_{v\perp}\simeq 2m_{e\perp}$. Equation (2) indicates that the E_1 (and also $E_1+\Delta_1$) transtions split into doublets as a result of the different confinement energies in the case of [110] superlattices. Obviously, this does not happen for [100]-oriented (tetragonal symmetry) superlattices.

Optical anisotropy for polarizations in the (110) plane ([1$\bar{1}$0],[001]) results from the fact that the two sets of ⟨111⟩ directions couple differently to the two principal polarization directions. This coupling can be easily estimated with the rule that only electric-field polarizations perpendicular to the ⟨111⟩ direction under consideration have nonzero matrix elements. The relative strengths obtained in this manner are listed in Table I.

The calculation is slightly more subtle in the absence of s.o. splitting ($\Delta_1=0$) because of the orbital degeneracy of the valence bands. The confinement shifts of the conduction bands are basically the same as for $\Delta_1\neq 0$ but the valence bands now split for $\mathbf{k}$ perpendicular to each ⟨111⟩ direction, leading to two different values of m_v^*: $m_v^*=m_c^*$ and $m_v^*=\infty$. The E_1 transitions thus split into four, although only three of them couple to the light (see Table I).

In Table I the calculated energy shifts for the two polarizations and their relative intensities are given. The calculations for ΔE refer to an infinitely high barrier and thus are expected to give values that largely exceed the experimentally observed ones. The purpose of the calculation is to show, on a simple basis, that due to the orthorhombic symmetry, a splitting of the E_1 transition is expected, with different intensities for the two polarizations. This is also what we observe experimentally, as depicted in Fig. 2, where the second derivative spectrum $d^2\epsilon_2/d\omega^2$ near E_1 of the 12 × 8 SL is shown. The second derivative has been used in order to emphasize the structure of the critical points responsible for the transitions, as is usual in ellipsometric analysis. The splitting of E_1 into a doublet is especially distinct for this sample, albeit also discernible in the other samples. The two small additional peaks which we find should correspond to the $E_1+\Delta_1$ transitions although crystal-field effects prevent us from considering the observed E_1, $E_1+\Delta_1$ as simply a spin-orbit doublet.

We also see qualitative agreement between the intensities of the E_1 doublet in Fig. 2 and the calculated ones

TABLE I. Relative intensities of the split E_1 transitions (that are shifted up in energy by ΔE with respect to the bulk values) for light polarized along the two main axes perpendicular to the growth direction. Results with and without spin-orbit (s.o.) coupling are given.

Polarization direction	With s.o. coupling			
	$\Delta E=1/4m_c(\pi/d)^2$	$3/4m_c(\pi/d)^2$		
[001]	$\frac{2}{3}$	$\frac{2}{3}$		
[1$\bar{1}$0]	1	$\frac{1}{3}$		
	Without s.o. coupling			
	$\Delta E=1/6m_c(\pi/d)^2$	$1/3m_c(\pi/d)^2$	$1/2m_c(\pi/d)^2$	$1/m_c(\pi/d)^2$
[001]	0	$\frac{2}{3}$	$\frac{2}{3}$	0
[1$\bar{1}$0]	1	0	$\frac{1}{3}$	0

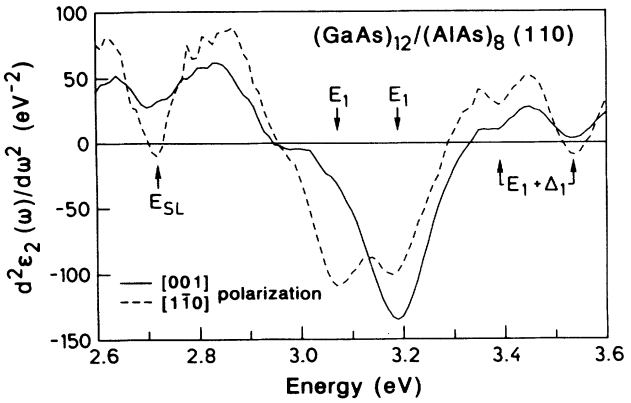

FIG. 2. Second derivative spectrum $d^2\epsilon_2(\omega)/d\omega^2$ of the $(GaAs)_{12}/(AlAs)_8$ SL for [001] polarization (full line) and [1$\bar{1}$0] polarization (dashed line).

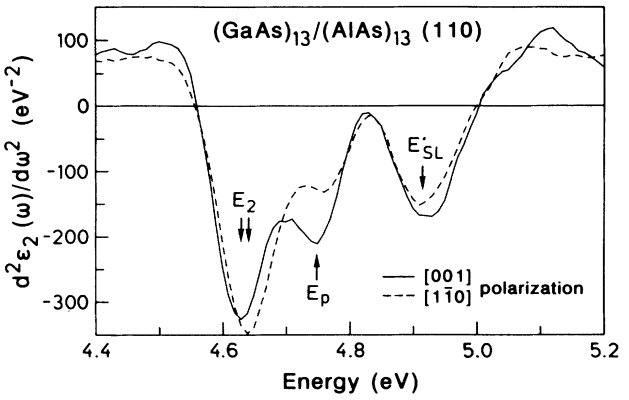

FIG. 3. As in Fig. 2 for the $(GaAs)_{13}/(AlAs)_{13}$ SL at higher energies.

in Table I, i.e., the amplitude of the energetically lower peak is larger for [1$\bar{1}$0] than for [001] polarization and vice versa for the higher-lying transition. The same level of agreement is found for the LMTO calculations of the 5 × 5 and 7 × 7 GaAs/AlAs SL, but the exact ratio of the intensities fluctuates heavily with the number of **k** points used in the evaluation of $\epsilon_2(\omega)$. For the exact representation of such details of the optical anisotropy it would thus be desirable to have an even denser **k** mesh in the calculation, but as mentioned above, this would require computing resources beyond our limits. Nevertheless, the *difference* of $\epsilon_2(\omega)$ in this energy region agrees well with experiment.

In addition to the E_1-derived transitions, we find somewhat weaker structures appearing below E_1 in both polarizations with approximately comparable intensities in all samples and calculations. In analogy to GaAs/AlAs SL's grown along the [001] direction, where such peaks have been found as well and attributed to the reduced symmetry compared to the bulk materials,[1] we also denote these transitions E_{SL}, as depicted in Fig. 2. They originate close to the point where the [110] direction of the orthorhombic BZ (which corresponds to the Δ direction of the bulk BZ) cuts through the surface of the orthorhombic BZ, involving transitions from the highest valence to the lowest conduction bands. The additional peak denoted E'_{SL} appearing above the E_2 shoulder [see Figs. 1(a) and 3] is related to transitions along the X direction of the orthorhombic BZ ([1$\bar{1}$0] of the bulk). Neither of these superlattice-specific transitions show, within the experimental error, any dependence on polarization. The structure labeled E'_1 is not present in the ellipsometric spectra due to the photon energy limitation.

The E_2 transitions show a small shift towards lower energies for the [1$\bar{1}$0] with respect to the [001] polarization. Fitting the critical points with a two-dimensional line shape,[7] these shifts amount to $\Delta E_2 = E_2^{[1\bar{1}0]} - E_2^{[001]} \approx 19$ meV up to $\approx$31 meV for total periodicities of $n + m = 10$ and $n + m = 20 - 26$, respectively. This compares rather favorably with the LMTO results of $\Delta E_2 \approx 20$ and 35 meV for the 5 × 5 and 7 × 7 structure, respectively. While this effect is rather small and not always discernible, especially in very-short-period SL's ($n + m \lesssim 12$), we observe an additional peak just above the E_2 edge that is unique (or at least predominant) for [001] polarization, and which was found in all samples. It disappears for light polarized along [1$\bar{1}$0] in what we believe to be the best samples. It is labeled E_p in Fig. 3, where $d^2\epsilon_2(\omega)/d\omega^2$ is shown for a $(GaAs)_{13}/(AlAs)_{13}$ sample. The LMTO calculations indicate that this transition stems from roughly the same region of the BZ that

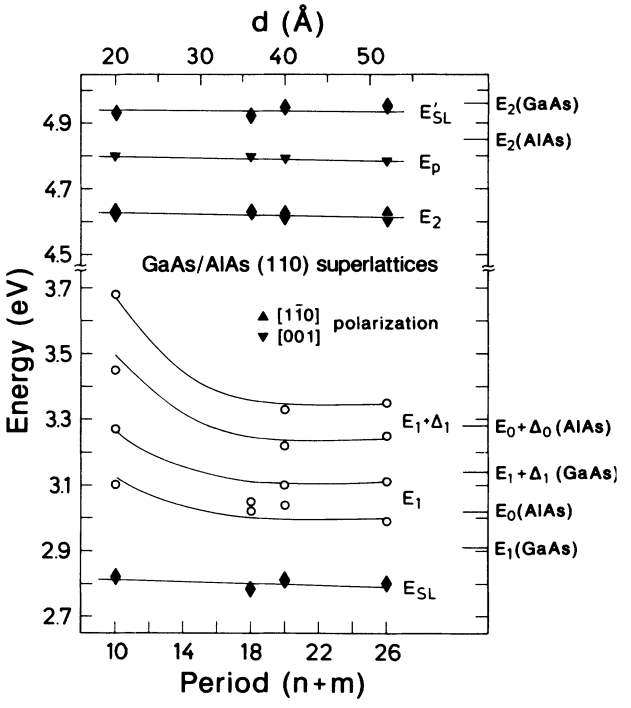

FIG. 4. Dependence of the various critical point energies on the superlattice period and polarization for [110] SL's with $n \approx m$. Diamonds represent transitions which are (within the experimental error) independent of polarization, in contrast to transitions for which triangles of different orientation have been used (see legend). The splitting of the E_1 and $E_1 + \Delta_1$ transitions due to the orthorhombic symmetry is indicated with ○. The lines are drawn through the experimental points as a guide to the eye.

accounts for E_{SL} but lower valence and higher conduction states are responsible for it.

Figure 4 summarizes the measured transition energies of the various critical points discussed above for $(GaAs)_n/(AlAs)_m$ SL's with varying superlattice period, expressed either as $(n+m)$ or the thickness d, and their polarization dependence. The samples shown have approximately the same GaAs and AlAs slab thickness ($n \approx m$, within 10%). The splitting of the E_1 critical point is displayed in this figure, as well as the polarization dependence of E_2. We observe most conspicuously that the energies of the E_1 and $E_1 + \Delta_1$ doublets increase as the superlattice period decreases. This can be qualitatively attributed to quantum confinement of the electronic or excitonic states. For the superlattice-related transitions E_{SL}, E'_{SL}, and E_p, this effect is negligible in the superlattice period range ($d = 52$ Å) examined. This is consistent with results obtained for GaAs/AlAs (001) SL's.[4]

It is interesting to compare the effects discussed above for the E_1 and $E_1 + \Delta_1$ transitions with those reported for the surface contribution to the dielectric function of GaAs. Calculations[27] and measurements[28] of the anisotropy of this surface contribution can be interpreted in a manner similar to that of Table I and Fig. 1(b). The differential surface response around E_1 (see Fig. 10 of Ref. 27) is qualitatively equivalent to the anisotropy found for the [110] SL's. It is possible to regard the surface anisotropy as a confinement effect in the surface layer (≈4 Å) induced by the barrier to vacuum and by the fact that the gap at the interface is on the average somewhat smaller than the bulk gap.

In summary, we have presented both experimental and theoretical results for the optical properties of GaAs/AlAs (110) SL's, and their optical anisotropy resulting from the orthorhombic symmetry of these SL's. Our simple model calculation accounts for the splitting of the E_1 transition into a doublet, and the experimental results are in qualitative agreement with both this model and the *ab initio* calculations. The usefulness of these calculations in spite of omitting s.o. coupling is supported by our simplified confinement model of the E_1 and $E_1 + \Delta_1$ transitions (Table I), which predicts only marginal changes for the full calculations that include s.o. coupling. The model also predicts qualitatively the anisotropy observed and calculated for the surface contribution to the dielectric function. The LMTO calculations and experiment are in good agreement in the description of the shift of the E_2 transitions for the two polarizations. The orientation of the SL's can be checked by analyzing the magnitude of the E_p transition, which has its maximum amplitude in [001] polarization. Similarities and differences between (001)- and (110)-oriented GaAs/AlAs SL's have been discussed. The optical properties of GaAs/AlAs (110) superlattices, as well as their anisotropy, are of basic physical interest and should become important for optoelectronic devices, such as optical modulators.

It is a pleasure to thank M.K. Kelly for valuable discussions and a critical reading of the manuscript and L. Tapfer for x-ray measurements. The computer program for the calculation of $\epsilon(\omega)$ has been written by M. Alouani, whom we also thank for his help. Calculations have been performed on the CRAY-YMP at Höchstleistungsrechenzentrum für Wissenschaft und Forschung, Jülich, Germany.

*Permanent address: Department of Solid State Physics, Faculty of Science, Masaryk University, Kotlářská, 61137 Brno, Czechoslovakia.

†Present address: University of Darmstadt, Material Science Department, D-6100 Darmstadt, Germany.

[1] M. Alouani, S. Gopalan, M. Garriga, and N.E. Christensen, Phys. Rev. Lett. **61**, 1643 (1988).

[2] J.-B. Xia and Y.-C. Chang, Phys. Rev. B **42**, 1781 (1990).

[3] E. Ghahramani, D.J. Moss, and J.E. Sipe, Phys. Rev. B **43**, 9269 (1991).

[4] M. Garriga, M. Cardona, N.E. Christensen, P. Lautenschlager, T. Isu, and K. Ploog, Phys. Rev. B **36**, 3254 (1987).

[5] J. Nagle, M. Garriga, W. Stolz, T. Isu, and K. Ploog, J. Phys. (Paris) Colloq. **48**, C5-495 (1987).

[6] J. Humlíček, F. Lukeš, K. Navrátil, M. Garriga, and K. Ploog, Appl. Phys. A **49**, 407 (1989); J. Humlíček, F. Lukeš, and K. Ploog, Phys. Rev. B **42**, 2932 (1990).

[7] S. Logothetidis, M. Alouani, M. Garriga, and M. Cardona, Phys. Rev. B **41**, 2959 (1990); S. Logothetidis, M. Cardona, and M. Garriga, *ibid.* **43**, 11 950 (1991), and references cited therein for the linear optical response of the bulk materials GaAs and AlAs and details of the spectroscopic ellipsometer.

[8] L.T.P. Allen, E.R. Weber, J. Washburn, and Y.C. Pao, Appl. Phys. Lett. **51**, 670 (1987).

[9] D. Kirillov and Y.C. Pao, in *Epitaxy of Semiconductor Layer Structures*, edited by R.T. Tung, L.R. Dawson, and R.L. Gunshor, Materials Research Society Symposium Proceedings No. 102 (MRS, Pittsburgh, 1988), p. 169.

[10] Z.V. Popović, M. Cardona, E. Richer, D. Strauch, L. Tapfer, and K. Ploog, Phys. Rev. B **40**, 3040 (1989).

[11] D. Gershoni, I. Brener, G.A. Baraff, S.N.G. Chu, L.N. Pfeiffer, and K. West, Phys. Rev. B **44**, 1930 (1991).

[12] W.I. Wang, J. Vac. Sci. Technol. B **1**, 630 (1983); Surf. Sci. **174**, 31 (1986).

[13] R. Eppenga and M.F.H. Schuurmans, Phys. Rev. B **38**, 3541 (1988).

[14] R.J. Gordon, Z. Ikonić, and G.P. Srivastava, Semicond. Sci. Technol. **5**, 269 (1990).

[15] D.M. Bylander and L. Kleinman, Phys. Rev. Lett. **59**, 2091 (1987); **60**, 472(E) (1988).

[16] N.E. Christensen, Solid State Commun. **68**, 959 (1988), and references cited therein.

[17] R.M.A. Azzam and N.M. Bashara, *Ellipsometry and Polarized Light* (North-Holland, Amsterdam, 1977).

[18] D.E. Aspnes, G.P. Schwartz, G.J. Gualtieri, A.A. Studna, and B. Schwartz, J. Electrochem. Soc. **128**, 590 (1981).

[19] D.E. Aspnes, J. Opt. Soc. Am. **70**, 1275 (1980).

[20] N.E. Christensen, Phys. Rev. B **30**, 5753 (1984).

[21] S.B. Zhang, M.S. Hybertsen, M.L. Cohen, S.G. Louie, and D. Tomanek, Phys. Rev. Lett. **63**, 1495 (1989); X. Zhu and S.G. Louie, Phys. Rev. B **43**, 14 142 (1991); R. Hott, *ibid.* **44**, 1057 (1991).

[22] S. Gopalan, N.E. Christensen, and M. Cardona, Phys. Rev. B **39**, 5165 (1989).
[23] M. Alouani, L. Brey, and N.E. Christensen, Phys. Rev. B **37**, 1167 (1988). As in this paper and in Ref. 1, we omitted spin-orbit (s.o.) coupling in the calculation of $\epsilon(\omega)$. The calculated spectra thus do not show the$(E_1 + \Delta_1)$ peaks. A calculation for the 1×1 structure with s.o. coupling, however, yields this structure in agreement with the experiment in Ref. 1.
[24] O. Jepsen and O.K. Andersen, Solid State Commun. **9**, 1763 (1971).
[25] U. Schmid, F. Lukeš, N.E. Christensen, M. Alouani, M. Cardona, E. Kasper, H. Kibbel, and H. Presting, Phys. Rev. Lett. **65**, 1933 (1990).
[26] M. Cardona, in *Atomic Structure and Optical Properties of Solids*, edited by E. Burstein (Academic, New York, 1972).
[27] F. Manghi, R. Del Sole, A. Selloni, and E. Molinari, Phys. Rev. B **41**, 9935 (1990).
[28] V.L. Berkovits, I.V. Makaraenko, T.A. Minashvili, and V.I. Safarov, Solid State Commun. **56**, 449 (1985).